

## Chapter 2

### RF Principles and Creation of Electron Beam

#### 2.1 Electromagnetic Waves and Resonant Cavity

In accelerator physics, all forces interacting with charged particles originate from electromagnetic fields. Electric and magnetic fields act differently on charged particles; electric fields play a significant role in particle acceleration while magnetic fields act on the particle trajectory. Hence, electromagnetic waves are useful for particle acceleration only if they exhibit electric field components in the direction of particle propagation. Relationships between electromagnetic field components where the medium is a vacuum in a charge free environment ( $\rho = 0$  and  $\vec{J} = 0$ ), are given by Maxwell's equations in mks units as [26]

$$\nabla \cdot \vec{E} = 0, \quad \nabla \times \vec{E} = -\frac{\partial \vec{B}}{\partial t}, \quad (2.1)$$

$$\nabla \cdot \vec{B} = 0, \quad \nabla \times \vec{B} = \mu\epsilon \frac{\partial \vec{E}}{\partial t}, \quad (2.2)$$

where  $\mu = \mu_0\mu_r$  and  $\epsilon = \epsilon_0\epsilon_r$  are the permeability and the permittivity of the medium. In our application, a radiofrequency (RF) field is used to accelerate charged particle and express solutions of Maxwell's equations in the form of RF-fields oscillating sinusoidally with a resonant frequency of  $\omega = 2\pi f$ . Then, the electric and magnetic fields can be expressed as  $\vec{E} \propto e^{i\omega t}$  and  $\vec{B} \propto e^{i\omega t}$  and Maxwell's equations in the case of a time-varying field becomes

$$\nabla \cdot \vec{E} = 0, \quad \nabla \times \vec{E} = -i\omega\vec{B} \quad (2.3)$$

$$\nabla \cdot \vec{B} = 0, \quad \nabla \times \vec{B} = i\omega\mu\epsilon\vec{E}. \quad (2.4)$$

Applying the curl operator to both sides of the second equation in (2.3) and substituting term  $\nabla \times \vec{B}$  by  $i\omega\mu\epsilon\vec{E}$ , we achieve  $\nabla \times (\nabla \times \vec{E}) = \omega^2\mu\epsilon\vec{E}$ . With the vector identity  $\nabla \times (\nabla \times \vec{A}) = \nabla(\nabla \cdot \vec{A}) - \nabla^2\vec{A}$ , we get  $\nabla(\nabla \cdot \vec{E}) - \nabla^2\vec{E} = \omega^2\mu\epsilon\vec{E}$  and according to (2.3), the first term becomes zero ( $\nabla \cdot \vec{E}$ ). The wave equation for the electric field can then be expressed as

$$\nabla^2\vec{E} + k^2\vec{E} = 0, \quad (2.5)$$

where the wavenumber  $k = (\omega/c)\sqrt{\mu\epsilon}$ . Similarly, the wave equation for the magnetic field may be written as

$$\nabla^2 \vec{H} + k^2 \vec{H} = 0. \quad (2.6)$$

Equations (2.5) and (2.6) are the general differential wave equations for electromagnetic waves.

### 2.1.1 Waveguide Principle

Introduction of appropriate boundary conditions to wave equations (2.5) and (2.6) results in longitudinal field components necessary to accelerate charged particles. To generate accelerating fields, a wave propagating along the  $z$ -axis in a conducting cylindrical pipe of infinite length is considered in cylindrical coordinates  $(r, \varphi, z)$  as indicated in Fig 2.1.

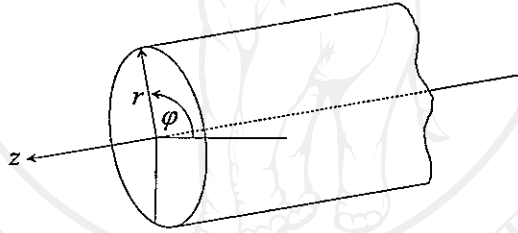


Figure 2.1. Infinite uniform circular metal waveguide.

In cylindrical coordinates, the  $z$ -component is the direction of particle propagation, the  $r$ -component is a radial direction and the  $\varphi$ -component is an azimuthal coordinate. The Laplacian of the wave vector in (2.5) and (2.6) may be split into Laplacian equations of the longitudinal and transverse components. The longitudinal component ( $z$ -component) of the electric and magnetic fields in (2.5) and (2.6) may be written as

$$\nabla^2 E_z + k^2 E_z = 0, \quad (2.7)$$

$$\nabla^2 H_z + k^2 H_z = 0. \quad (2.8)$$

The differential equations for the  $z$ -component of the electric and magnetic fields in cylindrical coordinates become

$$\frac{\partial^2 E_z}{\partial r^2} + \frac{1}{r} \frac{\partial E_z}{\partial r} + \frac{1}{r^2} \frac{\partial^2 E_z}{\partial \varphi^2} + \frac{\partial^2 E_z}{\partial z^2} + k^2 E_z = 0 \quad (2.9)$$

$$\frac{\partial^2 H_z}{\partial r^2} + \frac{1}{r} \frac{\partial H_z}{\partial r} + \frac{1}{r^2} \frac{\partial^2 H_z}{\partial \varphi^2} + \frac{\partial^2 H_z}{\partial z^2} + k^2 H_z = 0. \quad (2.10)$$

Due to symmetry considerations, the field pattern must repeat itself on turning azimuthally through an angle  $\varphi = 2\pi$ , thus a sinusoidal variation of the field is expected being periodic in  $\varphi$  and following a dependence like  $e^{in\varphi}$ , where  $n$  is an integer. Hence, the longitudinal electric field solution in (2.9) can be expressed as

$$E_z = E_0 \psi_r(r) \psi_\varphi(\varphi) \psi_z(z) e^{i\omega t} = E_0 \psi_r(r) E^{i(\omega t - n\varphi - k_z z)}, \quad (2.11)$$

where  $k_z$  is the propagation wavenumber. Applying the derivatives  $\partial^2/\partial^2\varphi = -n^2$  and  $\partial^2/\partial^2 z = -k_z^2$  to equation (2.9), then equation (2.9) may be written as

$$r^2 \frac{\partial^2 E_z}{\partial r^2} + r \frac{\partial E_z}{\partial r} - (k_c^2 r^2 - n^2) E_z = 0, \quad (2.12)$$

where  $k_c$  is a cutoff wavenumber defining the cutoff condition for the waveguide cross-section. This wavenumber is defined by

$$k_c^2 = k^2 - k_z^2 = \omega^2 \mu \varepsilon - k_z^2. \quad (2.13)$$

The nature of the parameters in equation (2.13) will determine whether the wave fields are usable for acceleration of charged particles. The wavenumber ( $k$ ) depends greatly on the angular frequency  $\omega$  and medium properties through the permeability ( $\mu$ ) and the permittivity ( $\varepsilon$ ) as  $k = \sqrt{\mu\varepsilon}(\omega/c)$ . Phase velocity ( $v_{ph}$ ) of the electromagnetic waves, which is the velocity of an observer riding along with the wave at a point of constant phase is given by

$$v_{ph} = \frac{\omega}{k_z} = \frac{\omega}{\sqrt{k^2 - k_c^2}}. \quad (2.14)$$

If there is no conducting boundaries, the cutoff wavenumber ( $k_c$ ) vanishes and the waves propagate for any frequency similar to a plane wave with the phase velocity of  $v_{ph} = \omega/k = c/\sqrt{\mu\varepsilon}$ . For the free space where  $\mu = \varepsilon = 1$ , the phase velocity becomes the speed of light ( $c$ ). Electromagnetic waves propagate in a conducting boundary only if the phase velocity is real ( $k > k_c$ ) and this is the reason why we call the quantity  $k_c$  as the cutoff wavenumber. For frequencies with a wavenumber less than the cutoff value ( $k < k_c$ ), the phase velocity becomes imaginary and the wave decays exponentially like  $e^{-\sqrt{k_c^2 - k^2}|z|}$  over a distance of a wavelength. The waves with frequencies above the cutoff frequency ( $\omega_c$ ) propagate along the axis of the hollow waveguide with a group velocity

$$v_g = \frac{d\omega}{dk_z} = \frac{c}{\sqrt{\mu\varepsilon}} \sqrt{1 - \left(\frac{k_c}{k}\right)^2} = \frac{c}{\sqrt{\mu\varepsilon}} \sqrt{1 - \left(\frac{\omega_c}{\omega}\right)^2}. \quad (2.15)$$

Equation (2.15) confirms the fact that the group velocity never exceeds the speed of light and a waveguide wavelength ( $\lambda_g$ ) defined as

$$\lambda_g = \frac{2\pi}{\sqrt{k_c^2 - k^2}}. \quad (2.16)$$

The second order differential in (2.12) has the form of  $x^2y'' + xy' + (a^2x^2 - n^2) = 0$ , which is known as Bessel's equation with solution of  $y = AJ_n(ax) + BY_n(ax)$  [27], where  $A$  and  $B$  are arbitrary constants of integration whose values are determined by the boundary conditions while  $J_n$  and  $Y_n$  are the *Bessel's functions* of order  $n$  of the first and second kind. Hence, the completed solution of the longitudinal electric field in (2.12) can be written as

$$E_z = [AJ_n(k_cr) + BY_n(k_cr)]e^{i(\omega t - n\varphi - k_z z)}, \quad (2.17)$$

where  $k_cr$  represents the cutoff position.

The electric field must be continuous and finite at the center of the waveguide so that no term in  $Y_n(k_cr)$  could be allowed to exist since  $Y_n(0)$  approaches  $-\infty$ , then the integration constant  $B$  must be zero. Lets assume that the circular waveguide shown in Fig.2.1 is a perfect conducting waveguide with a radius of  $a$ . The component of the electric field tangential to the wall must be zero at the boundary. The  $\varphi$ -component is always directed tangentially to the circular cross-section of the waveguide. Thus,  $E_\varphi$  and  $E_z$  must both be zero at the boundary,  $r = a$ , and  $AJ_n(k_cr) = 0$ . The integration constant  $A$  in equation (2.17) cannot be zero since it represents the field amplitude ( $E_0$ ) along the  $z$ -axis and therefore  $J_n(k_cr) = 0$ . Then, the expression for the longitudinal electric field  $E_z$  becomes

$$E_z = E_0 J_n(k_cr) e^{i(\omega t - n\varphi - k_z z)}. \quad (2.18)$$

The longitudinal electric field in (2.18) has a positive group velocity and propagate in positive  $z$ -direction. On the contrary, if the longitudinal field  $E_z \propto e^{ik_z z}$ , then it has a negative group velocity and travels in negative  $z$ -direction. Maxwell's equations do not provide any other connection between  $E_z$  and  $H_z$  so that they are independent variables. Relationship between the transverse field components from Maxwell's curl equations can be used to evaluate the transverse field components as

$$E_r = \frac{i}{k_z^2 - \mu\epsilon\omega^2/c^2} \left( k_z \frac{\partial E_z}{\partial r} + i \frac{\mu n}{r} H_z \right) \quad (2.19)$$

$$E_\phi = \frac{i}{k_z^2 - \mu\epsilon\omega^2/c^2} \left( ik_z \frac{n}{r} E_z - \mu\omega \frac{\partial H_z}{\partial r} \right). \quad (2.20)$$

$$H_r = \frac{-i}{k_z^2 - \mu\epsilon\omega^2/c^2} \left( i \frac{\omega\epsilon n}{r} E_z - k_z \frac{\partial H_z}{\partial r} \right) \quad (2.21)$$

$$H_\phi = \frac{i}{k_z^2 - \mu\epsilon\omega^2/c^2} \left( \omega\epsilon \frac{\partial E_z}{\partial r} + ik_z \frac{n}{r} H_z \right). \quad (2.22)$$

There are two different kinds of field configurations depending on the fields existing in the waveguide; transverse magnetic modes (TM-modes), with waves containing only electric field in the direction of propagation and transverse electric modes (TE-modes), with waves containing only magnetic field in the direction of propagation. The modes are identified by indices  $n$  and  $m$ . The index  $n$  is the order of the Bessel function and it is a measure of the circumferential variation in the field pattern while  $m$  is the  $m^{\text{th}}$  root of the Bessel function of order  $n$  and hence it is a measure of the radial variation of the field pattern. Equation (2.18) is the expression for the longitudinal electric field of the  $\text{TM}_{nm}$ -mode with the field amplitude  $E_0$  in (2.18) is a free variable, which can be determined by the power amplitude of an applying RF-wave. For the TE-modes, the longitudinal electric field  $E_z$  is zero everywhere throughout the inside of the waveguide and these modes are not suitable for particle acceleration. In theory, the waves will propagate inside conducting wall and are unaffected by anything outside the boundary. Practically, there is no perfect conducting material, so that the boundary is made of a finite high conductivity metal, such as, copper, silver, aluminum or brass. In this case, as the wave propagates along a hollow waveguide, attenuation of the wave will occur due to losses associated with the finite conductivity of the waveguide walls. In addition, if the waveguide is filled with a low loss material, there will be a contribution to the losses. The attenuation constants due to both effects may be calculated separately and then added to give the total attenuation constant. When the waveguide is filled with air, or is evacuated the losses may be neglected and wall losses will dominate.

### 2.1.2 Resonant Cavity

The waveguide modes discussed in section 2.1.1 are not a proper choice for particle acceleration because its phase velocities appearing to be larger than the speed of light. To make the phase velocity to become irrelevant, the principle

of two waves travelling in opposite directions on the same axis of a waveguide is used. The superposition of two equal but opposite waves form a *standing wave* with nodes half a waveguide wavelength ( $\lambda_g/2$ ) apart. Placing a conducting plate at such points inside the waveguide fulfills boundary conditions for an accelerating cavity. Inside the cavity, particles propagate along the  $z$ -direction and gain energy from the electrical accelerating fields. The cavity can be excited with different frequencies resulting in different modes. Dimensions of the cavity are designed such that the desired frequency is obtained. A practical and simple cavity shape is a short cylindrical box in form of a pillbox of radius  $a$  with length  $d$  as illustrated in Fig.2.2.

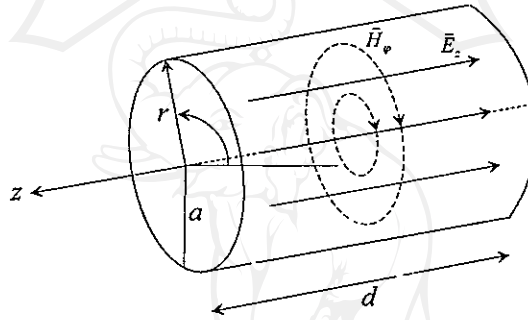


Figure 2.2. Pillbox cavity of radius  $a$  and length  $d$  with electromagnetic field lines in the  $TM_{010}$ -mode.

To make the cylindrical conducting tube to be the pillbox cavity, we place conducting end caps at positions  $z = \pm d/2$  to terminate the fields in the tube. This allows us to establish a standing wave pattern inside the cylindrical box. If particles are allowed to enter and exit the pillbox cavity, for instance, by two small holes in the conducting end plates, they can be accelerated by the longitudinal electric field. The total field from equation (2.18) becomes  $E_z = E_0 J_n(k_c r) e^{i(\omega t - n\varphi)} [e^{-ik_z z} + e^{ik_z z}]$ . The waves with positive group velocity ( $E_z \propto e^{-ik_z z}$ ) are called *forward waves* while the waves with negative group velocity ( $E_z \propto e^{ik_z z}$ ) are *backward waves*. We extend the nomenclature of waveguide modes to cavity modes by adding a third index for the eigenvalue  $p$  leading to a  $TM_{nmp}$ -mode resonant cavity. The index  $p$  represents a field variation in the longitudinal  $z$ -direction and  $k_z = p\pi/d$ . Then, the cutoff wave number in equation (2.13) becomes

$$k_c^2 = \mu\epsilon\omega^2 - \frac{p^2\pi^2}{d^2}. \quad (2.23)$$

The location of the cylindrical boundary is determined by the roots of the Bessel's function of order  $n$ . At the same frequency ( $\omega$ ), the waves in all modes propagate with the same group velocity. For efficient acceleration the particles and the wave should have the same velocity ( $v_p = v_{ph}$ ) and the synchronous condition will be fulfilled. The lowest TM-mode with the indices  $n$  and  $p$  both zero is the  $TM_{010}$ -mode. The lowest order root is obtained for  $k_c r = 2.405$  and the walls of the waveguide must be at  $a = (2.405\lambda_c)/(2\pi)$ . Expressions in equations (2.19)-(2.22) provide the conclusion that there is no transverse electric field as well as no radial and longitudinal magnetic field in the  $TM_{010}$ -mode since the index  $n$  and  $p$  are zero at  $a = 2.405/k_c$ . Deriving the longitudinal electric field for the  $TM_{010}$ -cavity from equation (2.18) and we obtained

$$E_z = E_0 J_0(2.405 \frac{r}{a}) e^{i(\omega t)}, \quad (2.24)$$

where  $\omega$  is an angular resonance frequency of the  $TM_{010}$ -mode and  $E_0$  is the peak electric field. The azimuthal magnetic field inside the  $TM_{010}$ -mode cavity, can be written as

$$H_\phi = \frac{i\omega\epsilon}{k_z^2 - \mu\epsilon\omega^2} \frac{\partial E_z}{\partial r} = -i(\epsilon_0 c) \sqrt{\frac{\epsilon}{\mu}} E_0 J_1(2.405 \frac{r}{a}) e^{i\omega t}. \quad (2.25)$$

The electric field configuration for this mode consists of a finite  $E_z$ -component parallel to the  $z$ -axis of the cavity and falling off transversely from a maximum value along the  $z$ -axis in the center of the cavity to be zero at the walls (Fig.2.3). The magnetic field circles around the  $z$ -axis and has no  $z$ -component (Fig.2.2).

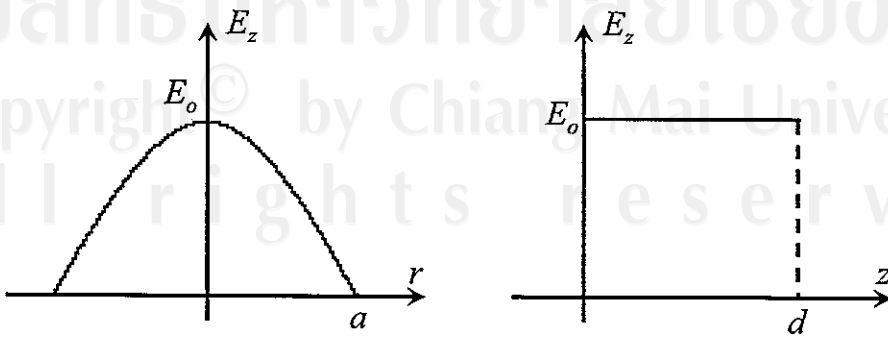


Figure 2.3. Electric field as a function of radius  $a$  and length  $d$  of the  $TM_{010}$ -mode pillbox cavity.

## 2.2 RF Cavity Parameters

Some basic theories corresponding to the resonant cavity parameters will be introduced in this section. Discussion of RF-parameters for the resonant cavity includes the resonant frequency, cavity radius and length, cavity wall losses, shunt impedance, quality factors and RF-coupling coefficient. Fundamental principle of an equivalent circuit for the resonant cavity as well as the principle of how to couple an external RF-power to the cavity will also be described in this section. The effects from the external source to the resonant cavity parameters will be discussed as well.

### 2.2.1 Resonant Frequency and Cavity Radius

The resonant frequency of the RF-cavity is required to meet the operating frequency of the input electromagnetic waves. Otherwise, the particles cannot be accelerated constantly throughout the cavity. To determine the resonant frequency is to observe the variation of the power delivered to the cavity. When the resonance occurs, the power output at the resonance significantly differs from the de-tuned conditions. For the  $TM_{010}$ -mode, which is used in almost all electric field accelerators, the resonant frequency is called the fundamental cavity frequency ( $f_0$ ) and it is inversely proportional to the cavity radius ( $a$ ) independent of the cavity length as

$$f_0 = \frac{\omega}{2\pi} = \frac{ck_c}{2\pi\sqrt{\mu\epsilon}} = \frac{2.405c}{2\pi\sqrt{\mu\epsilon}a}. \quad (2.26)$$

The appropriate resonant frequency for the cavity depends on the desired parameters for the particular application. At low resonant frequencies the particle bunch length is longer and also reduces the particle density in the bunch. In our case, we are interested especially in short bunches and high intensity particle beam, therefore high resonant frequency is suitable. The S-band cavity at a resonant frequency of 2856 MHz becomes our choice. The radius of a pillbox cavity can be defined from equation (2.26), which gives the cavity radius for the  $TM_{010}$ -mode resonant at the resonant frequency  $f_0$  in the free space where  $\mu = \epsilon = 1$  as

$$a = 2.405 \frac{c}{2\pi f_0}. \quad (2.27)$$



### 2.2.2 Energy Gain in RF-cavity and Transit Time Factor

Energy gain and accelerating voltage in the resonant cavity can be derived from the longitudinal accelerating field ( $E_z$ ). The longitudinal electric field along the  $z$ -axis inside the  $TM_{010}$  RF-cavity can be written as  $E_z = E_0 \sin(\omega t + \delta)$ . Assume the cavity center located at  $z = 0$  and a particle entering the cavity at position  $z = -d/2$  with phase  $\delta$  when it passes the cavity center. The particle gains energy while it travel through the resonant cavity with velocity  $v$ . By integrating the time dependent electric field along the travelling path, the kinetic energy gain of the particle may be expressed as [28]

$$\Delta E_{kin} = e \int_{-d/2}^{+d/2} E_z dz = eE_0 \int_{-d/2}^{+d/2} \sin\left(\frac{\omega z}{v} + \delta\right) dz. \quad (2.28)$$

The integral in equation (2.28) is maximum at  $\delta = \pi/2$  when the RF-field reaches its maximum amplitude at the time that the particle travels half way through the cavity. Hence, the kinetic energy gain of the particle becomes

$$\Delta E_{kin} = eE_0 d \frac{\sin(\omega d/2v)}{\omega d/2v} = eE_0 d T, \quad (2.29)$$

where  $T = \sin(\omega d/2v)/(\omega d/2v)$  which provides the correction on the particle acceleration due to the time variation of the field while the particle traverses the cavity and it is called the *transit-time factor*. As the transit-time factor of the cavity depends on the cavity accelerating length, it can be adjusted by varying the cavity length or the accelerating gap of the cavity. In order to achieve a maximum energy gain for a particle travelling approximately at the speed of light in the pillbox cavity of length  $d$  the transit-time factor of the pillbox cavity becomes  $T_{pillbox} = \omega d/2v = 2/\pi$ .

### 2.2.3 Accelerating Voltage and Accelerating Fields

The maximum accelerating field in the cavity depends on the power dissipation in the cavity and on the input power from external power source. A definition of a maximum voltage across the cavity ( $V_{cy}$ ) of length  $d$  is defined as

$$V_{cy} = \left| \int_0^d E_z dz \right|. \quad (2.30)$$

Hence, the maximum accelerating voltage for the  $TM_{010}$  RF-cavity of length  $d$  relates to the longitudinal electric field by  $V_{cy} = E_0 d T = 2E_0 d/\pi$  where the

transit time factor for the maximum acceleration is  $2/\pi$ . An average accelerating electric field that electron sees during its transit through the pillbox cavity of length  $d$  is given by

$$E_{ave} = \frac{V_{cy}}{d} = \frac{2E_0}{\pi}. \quad (2.31)$$

The ratio of the peak fields ( $E_0$ ) to the average accelerating fields ( $E_{ave}$ ) can be used to determine the maximum of acceleration as

$$\frac{E_{peak}}{E_{ave}} = \frac{E_0}{E_{ave}} = \frac{E_0 d}{V_{cy}} = \frac{\pi}{2} = 1.57. \quad (2.32)$$

#### 2.2.4 Length of Cavity

To make the cavity suitable for particle acceleration the cavity length must be optimized. To limit the interaction of RF-field and particle to the accelerating cycle only, the time a particle takes to traverse the pillbox cavity of length  $d$  is equal to half of an RF-period

$$t = \frac{d}{\beta c} = \frac{1}{2} T_{rf} = \frac{\pi}{\omega}. \quad (2.33)$$

For the  $TM_{010}$ -mode, there is only a standing wave inside the pillbox cavity of length  $d$ . Hence, the cavity length is related to the cavity wavelength ( $\lambda_{rf}$ ) like

$$d = \beta \frac{c\pi}{\omega} = \beta \frac{\lambda_{rf}}{2}, \quad (2.34)$$

where  $\beta = v/c$  while  $v$  is the velocity of the particle and  $\beta \approx 1$  for a particle travelling approximately at the speed of light. The relation of the cavity wavelength and the resonant frequency can be written as  $\lambda_{rf} = c/f_0$ . If the cavity is longer than the value calculated from equation (2.34), the particle sees some decelerating fields resulting in some deceleration. On the other hand, if the cavity is shorter, the particle does not gain as much energy as it could.

#### 2.2.5 Cavity Wall Losses and Shunt Impedance

The resonant cavity is normally made of highly conductive metal walls at proper boundary conditions. When there is no external RF-source connected to the cavity, the RF-fields will penetrate into the cavity wall to a depth which

is called the *skin depth*. Fields are lossless in a perfect conductor wall and the excitation of a cavity would maintain perfectly. In non-perfect conducting surface, the finite resistance of the material causes surface currents to produce heating losses leading to energy gain limit. These surface currents are induced from the azimuthal magnetic field component in the cavity wall and decay in the conducting wall surface. To contain the RF-fields within the conducting surface of the cavity, the electric surface currents, induced by these RF fields, are oriented such that they oppose the RF-fields, thus terminating the expansion of the RF fields into the wall. The surface currents can be derived from the Maxwell's curl equation of the azimuthal magnetic field ( $H_\phi$ ). The penetration depth of the electromagnetic fields and surface currents into the wall surface or the skin depth is defined by [29]

$$\delta_s = c \sqrt{\frac{2\epsilon_0}{\mu_s \omega \sigma_s}}, \quad (2.35)$$

where  $\mu_s$  and  $\sigma_s$  are the permeability and conductivity of the wall material, respectively. The skin depth depends greatly on material properties. The most popular material for constructing the resonant cavity is copper due to its high conductivity and low cost. The skin depth at 2856 MHz for copper with the resistivity  $\rho_s = 1.72 \mu\Omega\text{-cm}$  and conductivity  $\sigma_s = 5.8 \times 10^7 (\Omega\text{-m})^{-1}$ , is  $1.24 \mu\text{m}$ . The definition of cavity losses or dissipated power ( $P_{cy}$ ) per unit wall surface area  $S$  is given by

$$\frac{dP_{cy}}{dS} = R_s j_s^2, \quad (2.36)$$

where  $j_s$  is the surface current and  $R_s$  is the surface *shunt impedance* of the cavity defined by

$$R_s = \frac{4\pi\epsilon_0}{\sigma_s \delta_s}. \quad (2.37)$$

Evaluating the integral over all interior surfaces of the cavity and the cavity power losses of the  $\text{TM}_{010}$  pillbox RF-cavity becomes

$$P_{cy} = (4\pi\epsilon_0) \frac{\omega \sigma_s \epsilon \mu_s}{16\pi \mu} E_0^2 \int J_1^2(2.405 \frac{r}{a}) dS, \quad (2.38)$$

where  $\epsilon_0$  is the vacuum permittivity and it is equal to  $8.854 \times 10^{-10}$  F/m. Integrating over the cylindrical wall with surface area  $dS_{wall} = 2\pi a dz$  we get the cavity wall losses for the cylindrical wall of the  $\text{TM}_{010}$  pillbox RF-cavity as

$$P_{cy}(wall) = (4\pi\epsilon_0) \frac{\omega \sigma_s \epsilon \mu_s}{8 \mu} V_{cy}^2 \frac{a J_1^2(2.405)}{d}. \quad (2.39)$$

Similarly, the integral over each of end cap is  $dS_{cap} = 2\pi r dr$  and the cavity wall losses for each end cap becomes

$$P_{cy}(cap) = (4\pi\epsilon_0) \frac{\omega\sigma_s\epsilon\mu_s}{16\mu} V_{cy}^2 \frac{a^2 J_1^2(2.405)}{d^2}. \quad (2.40)$$

The total cavity wall losses is the summation of  $P_{cy}(wall)$  and  $2P_{cy}(cap)$  from equations (2.39) and (2.40). The total cavity losses can be written in term of *cavity shunt impedance* and the accelerating voltage as

$$P_{cy} = \frac{V_{cy}^2}{2R_s}. \quad (2.41)$$

Thus, we can adjust the strength of the longitudinal electric field  $E_0$  to vary the cavity losses power. The cavity shunt impedance including the transit-time factor can be written as [28]

$$R_s = \frac{4\mu d^2}{(4\pi\epsilon_0)\omega\sigma_s\epsilon\mu_s a(a+d) J_1^2(2.405)} \left( \frac{\sin(\omega d/2v)}{\omega d/2v} \right)^2. \quad (2.42)$$

Often, the shunt impedance per unit length or the *specific shunt impedance*,  $r_s$ , is used and the cavity power losses becomes

$$P_{cy} = \frac{V_{cy}^2}{r_s d}, \quad (2.43)$$

where the specific shunt impedance is  $r_s = 2R_s/d$  and  $d$  is the total length of the cavity producing the accelerating voltage  $V_{cy}$ . Equation (2.43) reveals that the higher the shunt impedance the more power (or energy)-efficient the RF-cavity becomes. To minimize the cavity losses for a given accelerating voltage, the shunt impedance should be large. Since the shunt impedance is proportional to the resonant frequency squared from the transit time factor term in equation in (2.42) to achieve high shunt impedance, high RF frequencies are preferred. Thus, for a fixed accelerating strength the shunt impedance is proportional to  $\sqrt{f}$ . In addition, the shunt impedance depends greatly on the cavity surface dimension and quality. We can optimize the geometric cavity parameters and surface quality to increase the shunt impedance and increase the transit-time factor of the cavity.

### 2.2.6 Quality Factor

The most importance parameter in a resonant system specifying the resonant frequency and performance is the *quality factor* or shortly called the  $Q$ -factor. It determines how the energy from the RF-source is split into cavity wall

losses and stored field energy. The Q-factor is defined as the ratio of the stored energy to the energy loss per RF-cycle [29]

$$Q = 2\pi \frac{\text{stored energy}}{\text{energy loss/cycle}} = 2\pi \frac{U}{T_{rf} P_{cy}} = \omega \frac{U}{P_{cy}}, \quad (2.44)$$

where  $U$  is the stored energy in the cavity and  $T_{rf}$  is the RF-cycle of oscillation. The stored energy is a volume integral of the squared electric and magnetic field. In the  $TM_{010}$ -mode there is only the longitudinal electric field in the particle propagating direction. Hence, the stored energy can be expressed as

$$U = (4\pi\epsilon_0) \frac{\epsilon}{8\pi} \int_V E_z^2 dV = \frac{4\pi\epsilon_0}{8} E_0^2 da^2 J_1^2(2.405), \quad (2.45)$$

Information of the resonant frequency, Q-factor and the shunt impedance is useful for the description of the resonant-cavity characteristics and their values can be measured experimentally. The Q-factor and shunt impedance depend greatly on the particular sources of loss in the cavity. If the shunt impedance represents the energy lost in the resonant system only, the quality-factor is called the *unloaded Q-factor*,  $Q_0 = \omega_0 U / P_{cy}$ , and  $P_{cy}$  is the power losses due to the cavity wall losses. If the resonant cavity is coupled to an external power source absorbing some amount of power, like an electron beam, an additional impedance is added to the system resulting in less shunt impedance and a smaller value of Q-factor. This Q-factor becomes the *loaded Q-factor*,  $Q_L = \omega_0 U / P_L$ , where  $P_L$  is the power losses in the cavity plus the losses due to the external system ( $P_L = P_{cy} + P_{ext}$ ). If the resonant cavity is loss-free and only loaded by the external system, the *external Q-factor*,  $Q_{ext} = \omega_0 U / P_{ext}$ , will be introduced to be the quality factor of the external system and  $P_{ext}$  is the power losses due to the external system. The loaded Q-factor of the cavity may be written in terms of the unloaded and the external Q-factors as

$$Q_L = \frac{\omega_0 U}{P_{cy} + P_{ext}} = \left( \frac{1}{Q_0} + \frac{1}{Q_{ext}} \right)^{-1}. \quad (2.46)$$

Equation (2.46) allows us to achieve the relation between these three quality factors  $Q_L$ ,  $Q_0$ , and  $Q_{ext}$  as

$$\frac{1}{Q_L} = \frac{1}{Q_0} + \frac{1}{Q_{ext}}. \quad (2.47)$$

When an external RF-field is applied to excite the resonant cavity, the excitation of the cavity may appear in a number of RF-modes, but in general only one

mode is near resonance. This idea leads to a well-known use of the  $Q$ -factor in describing bandwidth of a resonant cavity mode. The  $Q$ -factor can be measured experimentally from the width of the resonance curve and its value depends greatly on point of view of loaded or unloaded system. Generally, the  $Q$ -factor value is desired to be high for lower power dissipation. The most significant factor limiting the  $Q$ -factor is the finite conductivity of the cavity walls which depends greatly on the skin depth  $\delta_s$ . If the conductivity is independent of the frequency, it can be concluded from equation (2.35) that the  $Q$ -factor is proportional to  $1/\sqrt{f_0}$ .

### 2.2.7 Resonant Cavity and Equivalent Circuit

For each RF-cavity mode, its RF-parameters can be described by using an equivalent RLC circuit [30]. Relation of the resonant cavity and the equivalent circuit parameters can be used to define RF-cavity characteristics. The equivalent circuit of the RF or microwave system cannot be described so explicit because we cannot apply the common concept of voltage and current from Ohm's law in a low frequency circuit to the RF-system. However, the equivalent circuit is useful in modelling of the resonant system.

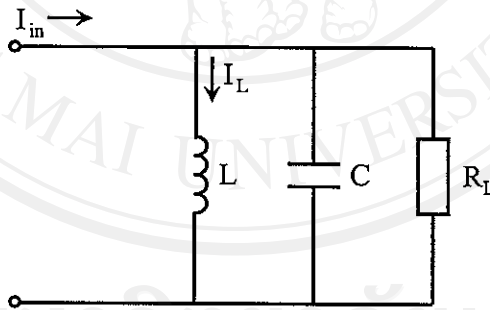


Figure 2.4. Equivalent RLC circuit for a resonant cavity.

Figure 2.4 illustrates a simple equivalent RLC circuit for resonant system with an input impedance of

$$Z = \left( \frac{1}{R_L} + \frac{1}{i\omega L} + i\omega C \right)^{-1}, \quad (2.48)$$

where  $R_L$  is the loaded resistance. When the input power generator is connected to the circuit with input current  $I_{in} = I_0 e^{-i\omega t}$ , magnetic field is stored in the resonant system by the current  $I_L$  through the inductor  $L$  and the electric field

is stored in the system by the accelerating voltage  $V_c$  across the capacity  $C$ . The resonance occurs when the average stored magnetic energy  $U_m = (1/4)L|I_L|^2$  is equal to the average stored electric energy  $U_e = (1/4)C|V_c|^2$  and the resonant frequency of the system may be written as

$$\omega_0 = \frac{1}{\sqrt{LC}}. \quad (2.49)$$

At resonance the input impedance of the circuit has only real components, so that from (2.48) the input impedance of the circuit will be equal to the loaded resistance ( $R_L$ ) of the circuit. From the expression in (2.44), the quality-factor of the system can be explained in terms of the  $R_L, L, C$  values as

$$Q_0 = \omega_0 \frac{(U_m + U_e)}{P_{cy}} = \frac{R_L}{\omega_0 L} = \omega_0 C R_L, \quad (2.50)$$

and the expression in (2.41) provides the relation of the shunt impedance ( $R_s$ ) in terms of the  $R_L, L, C$  values as

$$R_s = \omega_0 Q_0 L = \frac{Q_0}{\omega_0 C} = \frac{R_L}{Q_0^2}. \quad (2.51)$$

Together with the definition of the Q-factor in (2.50), the shunt impedance of the resonant system becomes  $R_L$  and in this case the voltage across the capacity ( $V_c$ ) is the effective voltage ( $V_{cy}$ ) across the cavity. Equations (2.49)-(2.50) show three universal relations of equivalent electrical circuit parameters ( $L, C, R_L$ ) and RF-parameters ( $\omega_0, Q_0, R_s$ ), which are used to characterize the behavior of the resonant system. The RF-cavity equivalent circuit is different from the common low-frequency circuit in two main points. First, the RF-cavity circuit parameters must be established separately for each resonant mode. Second, the shunt impedance  $R_s$  is not the common resistance as described by the relation of voltage and current in *Ohm's law*. It is defined in terms of the integration peak axial-electric field ( $\vec{E}_z$ ) along the cavity path and the power dissipated in the cavity wall ( $P_{cy}$ ) as

$$R_s = \frac{V_{cy}^2}{2P_{cy}} = \frac{|\int_0^d E_z dz|^2}{2P_{cy}}. \quad (2.52)$$

### 2.3 RF Coupling to Resonant Cavity

To excite the resonant cavity, the electromagnetic waves must be applied externally to couple in and out from the cavity. The coupling from external source

changes the characteristics of the resonant system. In this section, the principle of an RF coupling from generator to the resonant system, the definition of an RF-coupling coefficient and the transient-time behavior of the resonant system will be discussed.

### 2.3.1 RF Coupling from RF-Generator to Resonant System

The coupling between the RF-power generator and the resonant system can be explained with an equivalent circuit as shown in Fig.(2.4). The RF-generator provides an input current  $I_{in}$  with its internal resistance to the resonant circuit, which leads to an additional loss to the resonant system. The resonance of the complete circuit (resonant system plus external generator) can be described by the *loaded quality factor*  $Q_L$  as

$$Q_L = \frac{Q_0 Q_{ext}}{Q_0 + Q_{ext}}. \quad (2.53)$$

The external  $Q_{ext}$  determines coupling coefficient of the external generator to the resonant system. If the external  $Q_{ext}$  is larger than the unloaded  $Q_0$  the system is over-coupled, and if it is smaller the system is under-coupled.

### 2.3.2 RF Coupling Coefficient

External electromagnetic waves cannot excite the resonant cavity if it is completely enclosed by the conductor wall. In our case, introduction of a hole or iris between the resonant cavity and a driving RF-input port is used to couple the RF-waves into the RF-gun, the hole is located such that some field components in the cavity have a common direction to the exciting field. The external RF-waves coupled to the cavity can be determined from a parameter called the *RF-coupling coefficient*,  $\beta_{rf}$ , which is defined as the ratio of the power loss in the external circuit to that in the RF-cavity. Since the loaded  $Q_L$  includes all energy loss for the entire system, while the unloaded  $Q_0$  includes only energy loss in the cavity itself the relation of these quality factors and the RF coupling coefficient ( $\beta_{rf}$ ) is given by [31]

$$\beta_{rf} = \frac{\text{power loss in external circuit}}{\text{power loss in RF cavity}} = \frac{Q_0}{Q_L} - 1. \quad (2.54)$$



Equation (2.54) reveals that if the loaded and unloaded  $Q$ -factors of the RF-cavity can be measured, the RF-coupling coefficient between the RF-source and the loaded RF-cavity can be determined as well. If  $\beta_{rf} = 1$ , the system becomes coupled and the cavity is matched to the power source at resonance (without beam). Then, the loaded quality factor  $Q_L = Q_0/2$ . If  $\beta_{rf} > 1$ , the system is over-coupled and for the under-coupled system  $\beta_{rf} < 1$ . Therefore, it is convenient to measure the degree of coupling between the external power and the cavity by specifying the unloaded  $Q_0$ , the loaded  $Q_L$ .

### 2.3.3 Transient-Time Behavior

In case of a RF-pulsed source, at the moment the RF-source is tuned on the fields inside the RF-cavity is still zero. It requires some time to build up the standing-wave fields inside the RF-cavity. The power  $P(t)$  flowing into the RF-cavity is the sum of the rate of change of the stored energy and the rate of change of power dissipation and can be written as

$$P(t) = \frac{dU(t)}{dt} + \frac{\omega_0 U(t)}{Q}. \quad (2.55)$$

In the first instance the RF-generator is tuned on, all the input power is used to increase the stored energy in the RF-cavity. Consequently, the dissipated power increases while the stored energy increases. A steady-state is reached when the dissipated power equals the input power.

To study the steady-state condition, we consider a closed cavity without any external power, the power loss can be defined as the rate of change of the stored energy as  $P = -(dQ/dt) = \omega_0 U/Q$ . Then, we can evaluate the formation of the stored energy from  $dU/U = -(\omega_0/Q)dt$ . Finally, the decay of the stored energy becomes  $U = U_0 e^{-t/\tau_{cv}}$ , where  $\tau_{cv} = 2\tau_U = 2Q/\omega_0$  is a decay time of stored energy [28]. The parameter  $\tau_U$  is well known as *cavity time constant* or *cavity filling time*;

$$\tau_U = \frac{Q}{\omega_0}. \quad (2.56)$$

The filling time constant describes the build up time of the RF-fields in the cavity in order to supply the appropriated RF-power.

### 2.3.4 Voltage Standing Wave Ratio (*VSWR*)

To determine the coupled property of the resonant system, the concept of *Voltage Standing Wave Ratio* (*VSWR*) is introduced. The *VSWR* is defined as the ratio of the maximum voltage ( $V_{max}$ ) and the minimum voltage ( $V_{min}$ ) as

$$VSWR = \frac{V_{max}}{V_{min}} = \frac{|V^+| + |V^-|}{|V^+| - |V^-|}, \quad (2.57)$$

where  $V^+$  and  $V^-$  are the amplitude of the incident and reflected waves, respectively. It has been suggested by Ginzton [31] that when the load impedance is purely resistive and  $Z_0$  is the impedance of the transmission line, the *VSWR* can be written into two forms; i).  $R_L > Z_0$  then  $VSWR = R_L/Z_0$  and ii).  $R_L < Z_0$  then  $VSWR = Z_0/R_L$ . This leads to the definition of the impedance at the maximum and minimum voltage as  $Z_0 \times VSWR$  for  $R_L > Z_0$  and  $Z_0/VSWR$  for  $R_L < Z_0$ . Hence, The value of the RF-coupling coefficient can be evaluated by measuring the *VSWR* at resonance depending on how the RF-system is coupled. If the system is over-coupled,  $\beta_{rf} = VSWR$  and if the system is under-coupled,  $\beta_{rf} = 1/VSWR$ . It is noted that the input impedance  $Z_0$  and the loaded impedance  $R_L$  are defined in equation (2.33).

## 2.4 Creation of Electron Beam

The main concerns in a charged particle accelerator are how to generate and accelerate particles. The particle acceleration with an radiofrequency fields (RF-field) is described in the Sec.2.1. In this section, I will review on basic principles and the performance limitations of particle emission process. The particle emission process and its source properties limit the beam energy and beam current that can be obtained. Since our application is an electron accelerator the discussion from now on will concentrate only on the electron case. The discussion includes categories of electron sources and related effects in particle emission, i.e., space charge effect, Richard-Dushman's law and Schottky's effect.

### 2.4.1 Electron Sources

Electrons in the valence shell of metallic material are not strongly attracted by the nucleus. They are only held in the metal by the attractive force of

positive ions. Electrons, which have kinetic energies higher than the potential energy barrier or so-called the *work function* ( $\Phi_w$ ) of the metal, can escape from the metal surface. Work function is the minimum energy required for an electron to escape from the metal. The work function depends on the material property, for example, it is about 4.5 eV for Tungsten (W) and 1.6 eV for a Barium-Strontium oxide material [32]. In electron accelerators, different electron emitters made of different materials are used depending on application. There are several kinds of electron sources, which play important role in electron accelerators. To categorize electron sources or in another word *electron guns*, depends on how we distinguish them. If the electron emission process from the cathode is the main consideration, then thermionic emission, photoemission and field emission can be considered. If we consider how to provide the accelerating fields to the electron sources there are two groups: the DC-gun and the RF-gun. The basic information about electron emission and acceleration of each type of the electron gun is discussed in the following paragraphs.

#### *i) Thermionic Emission Electron Source*

Sir Owen W. Richardson was awarded the Physics Nobel Price in 1928 for revealing the thermionic emission phenomenon. He explained thermionic emission in terms of electrons evaporating from a hot metal surface. Electrons near the surface can escape from the metal surface if they have enough kinetic energy, which is derived from the heating temperature of the metal to overcome the attractive force of positive ions in the nucleus. Thermionic emission in an electron source starts when an electron emitter or cathode is heated. Electrons inside the cathode surface are moving with an average velocity controlled by the heating temperature. Some electrons having kinetic energies higher than the work function of the cathode material can escape from the cathode surface with thermal energy. These electrons form an electron beam when they emerge into a vacuum tube or an accelerating cavity, depending on particular application. Since the velocity of electron increase with the heating temperature, the number of electrons with sufficient energies to escape from the cathode surface also increases with temperature. Hence, higher heating temperature provides more electrons emitted from the cathode.

The energies of electrons emerging from the cathode depend on the cath-

ode temperature as

$$E_{kin} = \frac{3}{2}kT, \quad (2.58)$$

where  $k$  is the Boltzmann's constant and  $T$  is the filament heating temperature. This leads to the conclusion that higher heating temperature produces higher energy electrons and more electrons boiling off the cathode. Thermionic emitters are used in electron tubes and in special electron guns, for example, in klystrons, in electron beam welding, in medical linac for radiation therapy and in accelerators for lepton production. There are two main types of electron gun that use the thermionic emission to extract electrons from the cathode; thermionic DC-gun and thermionic RF-gun.

The thermionic DC-gun consists of two main parts. The first part is a heating filament, which consists of a piece of wire made of a resistive material and heated by an electric field. The tungsten is mainly used as a heated filament in the thermionic DC-guns. However, in modern technology different types of the cathode filament can be used depending on user applications. The second part is an accelerating region, which is bounded by two electrodes, known as cathode and anode. Electrons leave the cathode surface by a thermionic emission process with very small energy according to the thermal energy. They drift to the surface of the cathode, into a region where there is a DC electric field, which accelerates them across the gap towards the anode passing through a hole in the anode, with a final energy determined by the applied voltage of the electrode. The output electron beam for the thermionic DC-gun is a continuous beam. Figure 2.5 shows a schematic diagram of a simple Thermionic DC electron gun.

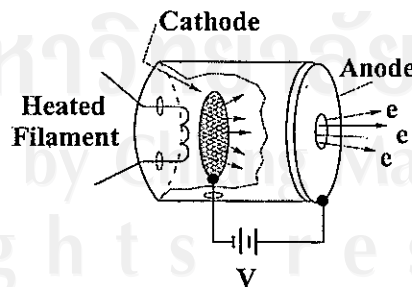


Figure 2.5. A schematic diagram of a simple Thermionic DC electron gun showing the cathode, the anode and the accelerating voltage  $V$ .

A thermionic RF-gun is an electron source consisting of a thermionic cathode serving as the electron emitter by the thermal emission process, which

emits electrons into the radio-frequency fields (RF-fields) inside a conducting walled cavity. When the RF-fields in the cavity are in the accelerating phase electrons are accelerated and leave the cathode with velocities depending on the magnitude of the RF-fields. In the thermionic RF gun, electron emission occurs continuously giving a train of bunches that varies in energy because of the time-varying RF-field.

*ii) Photo Emission Electron Source*

Photons illuminating a metal surface also liberate electrons. If the photon has an energy equal to or higher than the work function of the material ( $E \geq \Phi_w$ ), then electrons are emitted. The photon energy ( $E$ ) is expressed in term of the frequency of light ( $f$ ), the wavelength ( $\lambda$ ) of the incident light, the velocity of light ( $c$ ) and the Plank's constant ( $h$ ) as

$$E = hf = \frac{hc}{\lambda}. \quad (2.59)$$

For short wavelength or high energy light, electrons are emitted with a kinetic energy or an initial velocity given by

$$\frac{1}{2}mv^2 = hf - e\Phi_w. \quad (2.60)$$

Normally these velocities are small compared to the work function of most materials. To obtain reasonable electron emission with normal photon wavelengths, a low work function cathode material is used. For intense electron beams application, intense light sources are required. For this reason the laser-driven cathode has been used widely in many photocathode electron sources. There are two types of electron sources that use the photoemission principle; photocathode DC-gun and photocathode RF-gun.

In the photocathode DC electron guns, electrons are emitted from a photocathode by a short laser pulse and then accelerated by the electric field between the cathode and the anode. They move across the accelerating field gap of the gun, which has a large DC potential, and leave the anode hole with the energies depending on the DC potential between the electrodes. While in the photocathode RF-gun, short bunches of electrons are generated by a laser pulse incident on a photocathode located inside an accelerating RF-cavity. The electron emission process depends on the laser injector to the cathode. The laser used to illuminate the photocathode should provide very short pulses, at the wavelength

corresponding to the photocathode spectral response. Given the photocathode quantum yield, the laser micropulse should carry enough energy to extract the desired charge and it should be synchronized to a determined phase of the RF-signal. Since the cavity is operated at a high accelerating field electrons bunches emerging from the photocathode can gain kinetic energy to be relativistic in a very short distance. The pulse format of this type of electron source is more flexible than that of conventional DC-gun and that of thermionic RF-guns. It depends essentially on the laser pulse format which can be varied over a wide range. Photocathodes can deliver much higher current densities than thermionic cathodes.

At SURIYA facility, a thermionic RF-gun is used as an electron source. The main advantage of an thermionic RF-gun is that the thermionic RF-guns operate with much higher accelerating fields than the traditional DC-guns. This leads to reduction of the space-charge forces near the cathode and makes it possible to extract and accelerate very high current beams directly from the cathode. Rapid acceleration of electrons greatly lessens space-charge effects resulting in emittance degradation. Moreover, the thermionic cathode can produce an electron beam with reasonably high intensity. Although, photocathode RF-gun is a promising source to generate a high brightness ultra short electron pulses [33], it involves the complex laser injector, a high energy multi section linac and bunch compression system at high financial cost. On the other hand, a thermionic cathode RF-gun with suitable compression system can play similar role at low electron beam energy to produce electron beams with a pulse duration in the femtosecond time scale with lower, yet experimentally significant electron intensities.

There are phenomena which effect the electron emission in the thermionic RF-gun. The first effect follows the Richardson-Dushman law which states that the current density of the thermionic emission is limited by the heating temperature. The second phenomenon is the Schottky effect, which is related to the accelerating electric field inside an RF-cavity. The external electric field close to the cathode will reduce the work function of the cathode material. The last effect is the Child-Langmuir space charge effect which describes the relationship between an electron current density and an applying accelerating voltage. Details of Richardson-Dushman's law with Schottky's correction and the Child-Langmuir Space Charge effect will be discussed in the following sections.

### 2.4.2 Richardson-Dushman's Law

In thermionic emission, thermal energy is the driving force to allow electrons, which have kinetic energies higher than the potential barrier, escape from the cathode surface. The current density of electrons per unit energy and per unit volume generating from this process can be derived from

$$j = \int en(E)v_x(E)dE, \quad (2.61)$$

where  $e$  is electric charge of electron,  $v_{(E)}$  is the velocity of electrons while they reach the potential barrier and  $n(E)$  is the electron density from the emission given by the product of the density of states function  $f(E)$  and the Fermi function  $g(E)$  as

$$n(E)dE = f(E)g(E)d(E) = \frac{8\sqrt{2}m_e\pi}{h^3} \frac{\sqrt{E}dE}{1 + e^{(\frac{E-E_F}{kT})}}. \quad (2.62)$$

From the kinetic energy relationship,  $E = m_e v^2/2$ , the electron density becomes

$$n(E)dE = \frac{8\pi}{h^3} \frac{m_e^3}{1 + e^{(\frac{E-E_F}{kT})}} \frac{v^2 dv}{2} \cong \frac{2m_e^3}{h^3} e^{-(E-E_F)/kT} 4\pi v^2 dv, \quad (2.63)$$

where the Fermi function is approximated by the Maxwell-Boltzmann distribution. The electron energy can be expressed as the function of the velocity components in  $x$ ,  $y$ , and  $z$  direction as  $E = \frac{1}{2}m_e v^2 = \frac{m_e}{2}(v_x^2 + v_y^2 + v_z^2)$ . Then, equation (2.61) becomes

$$j = \frac{2em_e^3}{h^3} e^{E_F/kT} \int_{-\infty}^{\infty} v_x e^{-\frac{m_e v_x^2}{2kT}} dv_x \int_{-\infty}^{\infty} v_y e^{-\frac{m_e v_y^2}{2kT}} dv_y \int_{v_{z,min}}^{\infty} v_z e^{-\frac{m_e v_z^2}{2kT}} dv_z. \quad (2.64)$$

The integration over  $v_z$  starts from the minimum velocity ( $v_{z,min}$ ) in the positive  $z$ -direction needed to overcome the potential barrier to infinity. Setting the minimum kinetic electron energy equal to the potential barrier height

$$E_{min} = e\Phi_w + E_F = \frac{1}{2}m_e v^2, \quad (2.65)$$

get

$$\int_{v_{z,min}}^{\infty} v_z e^{-\frac{m_e v_z^2}{2kT}} dv_z = e^{-\frac{m_e v_{z,min}^2}{2kT}} \left(\frac{kT}{m_e}\right) = e^{-\frac{-e\Phi_w + E_F}{kT}} \left(\frac{kT}{m_e}\right), \quad (2.66)$$

while the integral over  $v_x$  and  $v_y$  extends from  $-\infty$  to  $+\infty$  and can be solved by using the definite integral:  $\int_{-\infty}^{\infty} e^{-t^2} dt = \sqrt{\pi}$ . Then, the second and third term in equation (2.64) become  $\sqrt{(2\pi kT)/m_e}$  and equation (2.64) becomes

$$j = \frac{4\pi em_e k^2}{h^3} T^2 e^{-\frac{e\Phi_w}{kT}}, \quad (2.67)$$

Hence, the current density for the thermionic emission may be written as

$$j = AT^2 e^{-\frac{e\Phi_w}{kT}}, \quad (2.68)$$

where  $A = 4\pi em_e k^2/h^3$  is a Richardson constant that is depending on the material properties, for example,  $A \approx 60 \text{ A}/(\text{cm}^2\text{-K}^2)$  for most metals,  $T$  is the temperature of the cathode,  $k$  is a Boltzmann constant ( $k = 1.381 \times 10^{-23} \text{ J/K}$ ), and  $\Phi_w$  is the work function of the cathode material. Equation (2.68) is well known as the Richardson's law or Richardson-Dushman's law providing the estimation of the current density from the thermionic emission. A numerical example for tungsten of work function of 4.5 eV with cathode heating temperature of about 2200 K, the maximum current density calculated from (2.68) becomes  $8.26 \times 10^{-2} \text{ A/cm}^2$ .

### 2.4.3 Schottky's Effect

While an external accelerating electric field is applied to the space around the cathode in a vacuum RF-cavity, the electric fields distort the potential barrier at the cathode surface resulting in a lower work function. This effect is called *Schottky effect* and was discovered by the German physicist Walter Schottky. The work function of the cathode material is reduced by the Schottky correction to the electric field as  $\Phi_w \rightarrow \Phi_w - \Delta\Phi$ . Hence, Richardson's law [34] becomes

$$j = AT^2 e^{-\frac{e(\Phi_w - \Delta\Phi)}{kT}}, \quad (2.69)$$

where  $\Delta\Phi$  is the Schottky's correction which is given by the quantum tunnelling through the work function barrier. The formation in (2.69) reveals that when the electric field is applied into the RF-cavity outside the cathode reduces the work function barrier of the cathode resulting in an increased electron beam current density.

### 2.4.4 Space Charge Effect and Child-Langmuir's Law

In the electrode structures, electrons emerging from the cathode surface feel an accelerating electric field and are accelerated off the cathode surface resulting in the lowering of the potential at the surface. A stable condition exists when the field is zero or at a constant potential. Any further electric field reduction would repel electrons back to the cathode. This stable regime is known as



*space-charge-limited emission.* The electron current density off the electron gun is limited by this space charge effect which is associated with the flow of charged particles in sufficient intensities to significantly change the potential in the region in front of the cathode that they drift through. This effect is governed by the Child-Langmuir's equation, which determines the maximum current of electrons that can be extracted from the cathode as a function of the accelerating voltage,  $V$ , defined as [35]

$$j = \frac{\chi}{d^2} V^{3/2}, \quad (2.70)$$

where a constant  $\chi = (4\epsilon_0/9)(2e/m)^{1/2}$  for electron of charge  $e$  and mass  $m$ . The perveance can be defined as a function of the electrodes geometry as  $P = \chi S/d^2$ , where  $S$  is a cathode emitting surface area and  $d$  is a spacing between electrodes. Figure 2.6 illustrating the relationship of the accelerating voltage and the electron current as a function of the heating temperature at the space charge limit.

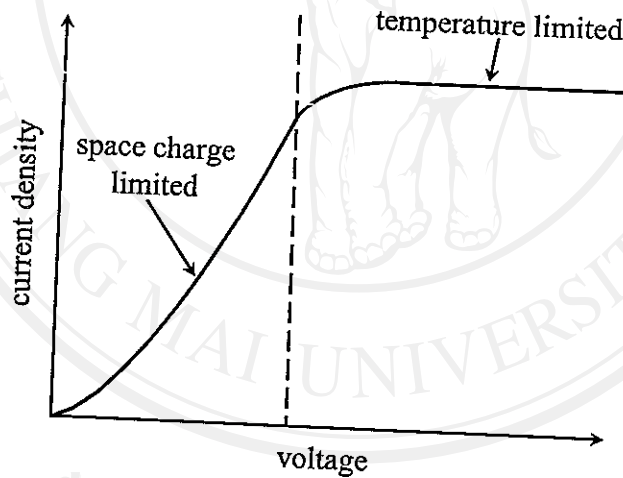


Figure 2.6. Thermionic emission regimes and space charged limited.

Calculations of the perveance  $\chi$  constant for electron with charge of  $e = 1.602 \times 10^{-19}$  C, rest mass of  $m_e = 9.109 \times 10^{-31}$  kg and the permittivity of vacuum is  $\epsilon_0 = 8.854 \times 10^{-12}$  Nm<sup>2</sup>/C<sup>2</sup> results in Child's constant as  $\chi = 2.334 \times 10^{-6}$  Nm<sup>2</sup>/Ckg or  $2.334 \times 10^{-6}$  A/V<sup>3/2</sup>. The space charge effect is not important in relativistic ion beams since it would have to carry the enormous power to reach relativistic energy. In our case the space charge effect only affects to the early state of electron emitting from the cathode with thermal energy of a few keV. In high gradient resonant cavity, this space-charge effect will be negligible when electrons are accelerated by the high RF-fields.

## 2.5 Time Structure and Beam Current Definitions

The time structure of a particle beam can be a continuous and a bunched beam. A continuous beam is a continuous flow of particles, which can be generated by DC accelerating field. In our application, a bunched beam is generated in an RF-gun due to the oscillating accelerating fields. Due to this oscillating fields electrons are accelerated in short microbunches separated by the RF-oscillation time. A series of such bunches is produced while the RF power delivers microwave energy and forms a pulsed beam consisting of a finite number of microbunches. In an electron accelerator, different electron currents can be defined; an average current, a pulse current and a peak current [28]. While all definitions are consistent with each other, the particular definition used depends on a particular experiment. The definitions for these currents will be introduced in this section.

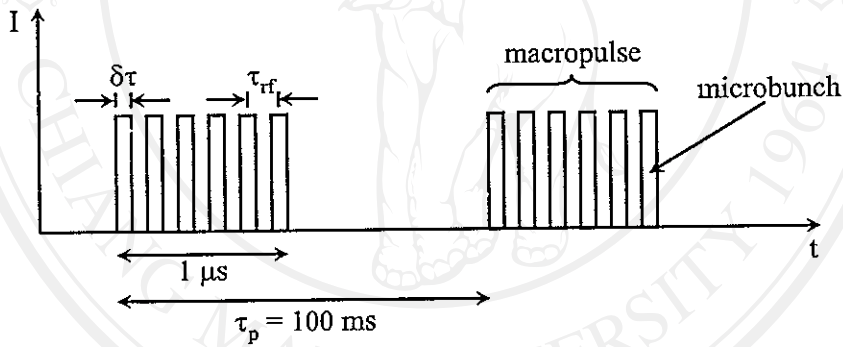


Figure 2.7. Time structure (schematic) of electron bunches and pulses.

### 2.5.1 Beam Current from Ohm's Law

The basic definition of the current is given by the amount of charge passing some point per unit time,

$$I = \frac{Q}{\Delta t}. \quad (2.71)$$

### 2.5.2 Peak Current

The microbunch current or the peak current is the instantaneous current in an electron bunch or in short it is the average current during the bunch defined

as

$$I_{peak} = \frac{q_b}{\delta\tau}. \quad (2.72)$$

where  $q_b$  is the total charge in the time interval  $\delta\tau$ .

### 2.5.3 Pulse Current

A series of  $N_b$  microbunches forms a beam pulse (macropulse) which is determined by the time duration of the RF-pulse. The pulse current is defined as the average current during the RF-pulse duration or the total charge per pulse duration. We derive the pulse current from the electric charge  $Q_p$  and the time duration  $\tau_p$  of each pulse. Hence, the pulse current from becomes with (2.72)

$$I_{pulse} = \frac{Q_p}{\tau_p} = \frac{N_b q_b}{N_b \tau_{rf}} = \frac{q_{bunch}}{\tau_{rf}}, \quad (2.73)$$

where  $\tau_{rf}$  is the the temporal time between the microbunches, which is defined from the resonant frequency ,  $q_b$  is the electric charge in an electron bunch,  $N_b$  is the number of the electron bunches per pulse. Generally, the pulse current is much less than the peak current because the temporal time between each bunch is much longer than the bunch length.

### 2.5.4 Average Current

The common definition of the electrical charge per unit time can be used to define the average current. For a bunched beam, the average beam current is the beam current averaged over long compared to the cycle of the accelerator. In terms of electrical charge  $Q$  and time  $t$ , the average current ( $I_{ave}$ ) can be expressed as

$$I_{ave} = \frac{Q}{t} = \frac{I_p \tau_p}{t}, \quad (2.74)$$

where total charge passing the current monitor during the time  $t \gg \tau_p$ . The average current is important for experiments that depend only on the total number of electrons accelerated per unit time independent of the actual time structure.

In our application, the RF-gun is energized by RF-pulses with a pulse width of a few  $\mu s$  at 10 Hz and produces therefore an electron beam for the same or shorter time duration. Assume that the macropulse is 1  $\mu s$  long and each pulse

is separated by 100 ms (1/10 Hz). Each macropulse contains about 3000 microbunches with 350 ps bunch separation determined by the RF-field frequency (2856 MHz). Figure 2.7 illustrates the common time structure of the bunched beams for the time scale described above.



ลิขสิทธิ์มหาวิทยาลัยเชียงใหม่

Copyright© by Chiang Mai University

All rights reserved